



**HAL**  
open science

## A Magnetic Monopole Antenna

Benoît Reynier, Xingyu Yang, Bruno Gallas, Sébastien Bidault, Mathieu Mivelle

► **To cite this version:**

Benoît Reynier, Xingyu Yang, Bruno Gallas, Sébastien Bidault, Mathieu Mivelle. A Magnetic Monopole Antenna. ACS photonics, 2023, 10 (9), pp.3070-3076. 10.1021/acsp Photonics.3c00423 . hal-04191014

**HAL Id: hal-04191014**

**<https://hal.sorbonne-universite.fr/hal-04191014v1>**

Submitted on 30 Aug 2023

**HAL** is a multi-disciplinary open access archive for the deposit and dissemination of scientific research documents, whether they are published or not. The documents may come from teaching and research institutions in France or abroad, or from public or private research centers.

L'archive ouverte pluridisciplinaire **HAL**, est destinée au dépôt et à la diffusion de documents scientifiques de niveau recherche, publiés ou non, émanant des établissements d'enseignement et de recherche français ou étrangers, des laboratoires publics ou privés.

# A magnetic monopole antenna

Benoît Reynier<sup>1</sup>, Xingyu Yang<sup>1</sup>, Bruno Gallas<sup>1</sup>, Sébastien Bidault<sup>2</sup> and Mathieu Mivelle<sup>1\*</sup>

<sup>1</sup> Sorbonne Université, CNRS, Institut des NanoSciences de Paris, INSP, 75005 Paris, France

<sup>2</sup> Institut Langevin, ESPCI Paris, Université PSL, CNRS, 75005 Paris, France

\*Corresponding author: mathieu.mivelle@sorbonne-universite.fr

ORCID:0000-0002-0648-7134

## Abstract

Magnetic monopoles are hypothetical particles which, similarly to the electric monopoles that generate electric fields, are at the origin of magnetic fields. Despite many efforts, to date, these theoretical particles have yet to be observed. Nevertheless, many systems or physical phenomena mimic the behavior of magnetic monopoles. Here, we propose a new type of photonic nanoantenna behaving as a radiating magnetic monopole. We demonstrate that a half-nanoslit in a semi-infinite gold layer generates a single pole of an enhanced magnetic field at the nanoscale and that this single pole radiates efficiently in the far field. We also introduce an effective magnetic charge using Gauss's law of magnetism, in analogy to the electric charge, which further highlights the monopolar behavior of this new antenna. Finally, we show that different plasmonic and metallic materials can provide magnetic monopole antennas covering the visible to near infrared range, and even down to GHz frequencies. This original antenna concept opens the way to a new model system to study magnetic monopoles and a new optical magnetic field source to study the "magnetic light-matter coupling". Furthermore, it opens potential applications at lower frequencies, such as in magnetic resonance imaging.

Keywords: Magnetic Monopole, Photonic Antenna, Plasmonics, Magnetic Field, Nanostructure.

## Introduction

Magnetic monopoles are hypothetical particles that carry a single magnetic pole, as opposed to all other magnetic objects that come in pairs of magnetic poles. The concept of magnetic monopoles was first proposed by Paul Dirac in the 1930s,<sup>1</sup> and has since been the subject of much theoretical and experimental research in the following decades.<sup>2</sup>

In many ways, magnetic monopoles are similar to electric charges. Just as electric charges are the fundamental building blocks of electric fields, magnetic monopoles are expected to be the fundamental building blocks of magnetic fields (figure 1). However, unlike electric charges, that exist as isolated entities, magnetic poles always come in pairs (north and south). Indeed, despite many experimental investigations, magnetic monopoles have yet to be unambiguously observed in Nature. Many physicists believe that they must exist in order to explain certain phenomena, such as the observed quantization of electrical charges.<sup>2</sup> In recent years, there have been several proposed methods<sup>3,4</sup> to investigate magnetic monopoles, including the use of high-energy particle accelerators, cosmic ray detectors, and the quest for magnetic monopole "tracks" in certain materials.

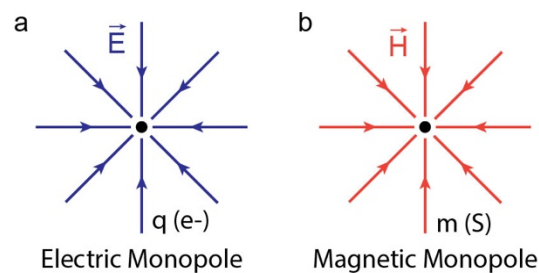


**Figure 1.** Description of electric and magnetic monopoles. a) A negative electric point charge generates electric field lines oriented in the direction of the charge. b) A south magnetic pole creates magnetic field lines in the direction of the pole.

Although magnetic monopole particles are yet to be observed experimentally, for many years, physicists have been trying to develop systems behaving like magnetic monopoles or have used the concept to explain the behavior of certain materials. This is the case, for instance, in topological insulators,<sup>5</sup> spin ice materials,<sup>6</sup> high-temperature superconductors,<sup>7</sup> during heavy ion collisions,<sup>8</sup> in quantum Hall systems,<sup>9</sup> skyrmions,<sup>10</sup> liquid crystals,<sup>11</sup> Weyl semimetals,<sup>12</sup> or chiral magnets,<sup>13</sup> to name a few. However, all these systems referring to the supposed behavior of magnetic monopoles are associated with a static behavior of the latter.

In electromagnetics, the concept of electric monopole is well known and well described in the scientific literature and is widely used technologically.<sup>14, 15</sup> At all electromagnetic frequencies, an electric monopole antenna consists in a conductive rod perpendicular to a conductive

surface that acts as a mirror or ground plane. The literature also refers to the existence of magnetic monopole antennas at GHz frequencies.<sup>16, 17</sup> However, the term magnetic monopole antenna in these studies is probably overstated as, to the best of our knowledge, the monopole behavior of these systems has never been investigated.

Therefore, to contribute to this endeavour, this paper proposes a new type of plasmonic nanoantenna, based on a half-nanoslit in a semi-infinite gold layer and behaving as a magnetic monopole. We demonstrate that our plasmonic nanostructure develops a single and enhanced magnetic hot spot at the nanoscale, which is locally free of any electric field. Furthermore, this enhanced energy density of optical magnetic field is made of only one orientation of the magnetic field, constituting a single pole, as opposed to plasmonic magnetic dipoles carrying two opposite poles, which locally amplify the magnetic field. Finally, we describe how this monopole oscillates in time at the excitation frequency, alternating north-south orientations, allowing this antenna to efficiently radiate electromagnetically in the far field from this single pole, similarly to how an electric monopole antenna would behave.

The results presented here are of great significance for several reasons. Firstly, this nanoantenna can be used as a model system to study the behavior of magnetic monopoles. Also, by its ability to concentrate, isolate and enhance the optical magnetic field at the nanoscale, this type of nanostructures opens new possibilities for manipulating the coupling between magnetic light and matter.<sup>18-27</sup> In particular, research topics where the optical magnetic field plays a major role, such as the interactions between light and chiral matter,<sup>28-30</sup> electrically forbidden photochemical processes,<sup>31</sup> or nonlinear photon avalanche processes involving the magnetic transitions of lanthanide ions,<sup>32</sup> will benefit directly from this type of system. Finally, owing to its efficient far-field radiation and ability to concentrate the magnetic field locally in the near-field, and similarly to other types of photonic antennas, the extension of this new concept to GHz and MHz frequencies will profoundly impact certain technologies such as magnetic resonance imaging.

## Results and discussions

In electromagnetism, antennas can feature a broad range of features<sup>33</sup> in terms of directivity, bandwidth, or gain. In the visible range, these structures, called nanoantennas,<sup>34</sup> have been developed in different types of materials, dielectric<sup>35-38</sup> or metallic,<sup>39, 40</sup> to cover a wide range of properties. Examples include fluorescence enhancement,<sup>41</sup> heat generation,<sup>42</sup> biosensing,<sup>43</sup> or directionality.<sup>44</sup> Many sophisticated antenna geometries have been used for these applications.<sup>44, 45</sup> However, some of the simplest nanoantenna geometries induce multipolar behaviors when they are excited by an optical field.<sup>46</sup> Figures 2a-c list some of these antennas. For instance, a gold nanorod (figure 2a) behaves like an electric dipole.<sup>47</sup> In particular, this

behavior leads to a strong enhancement of the optical electric field ( $\mathbf{E}$ ) at both ends of the nanorod when it is excited at resonance by a light polarized with the electric field collinear to the long axis of the antenna (figure 2a). Also, by reciprocity and via Babinet's principle, a nanoslit in a gold layer (figure 2b) behaves like a magnetic dipole.<sup>48, 49</sup> In this case, the optical magnetic field ( $\mathbf{H}$ ) is enhanced at the ends of the nanoslit, at resonance, for an excitation polarization with a magnetic field that is collinear to the antenna's long axis (figure 2b). Similarly, it has been demonstrated that a metal half-nanorod attached to a semi-infinite layer of the same metal (figure 2c) behaves like an electric monopole,<sup>15</sup> this time with a single electric hot spot at the end of the half-nanorod (figure 2c). From then on, by reciprocity and via the same Babinet principle, one can wonder whether the electromagnetic behavior of a half-nanoslit in a semi-infinite layer of metal is similar to a magnetic monopole which would generate only one magnetic hot spot (one pole) at the end of it (figure 2d). This paper numerically demonstrates this property in comparison to the behavior of the magnetic dipole (See Figure S2 of the Supporting information for comparison with electric monopoles and dipoles via the Babinet principle).

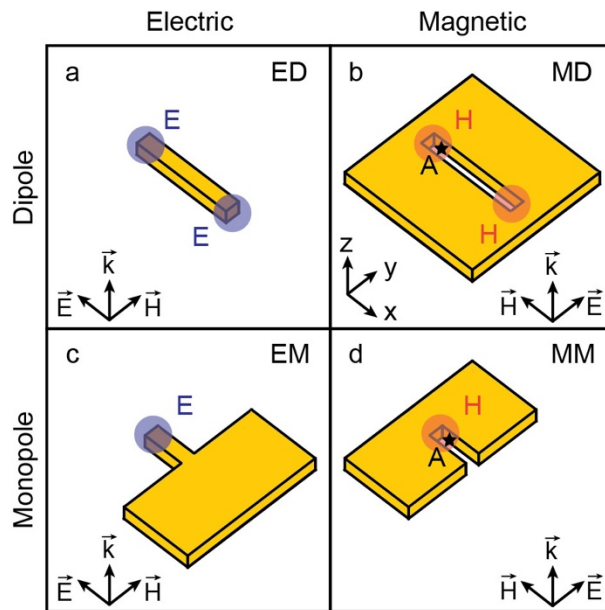


**Figure 2.** Schematic illustration of different plasmonic multipolar antennas. Design of dipolar a) electric, b) magnetic and monopolar c) electric, d) magnetic nanoantennas.

For this purpose, in this work, two structures are considered. One consists of a nanoslit drilled in a thin layer of gold, hereafter called the magnetic dipole, shown in figure 2b, and the other is a half-nanoslit in a semi-infinite layer of gold, hereafter called the magnetic monopole and shown in figure 2d. These two nanostructures are both made in a 40 nm thick gold layer, and their groove width is 20 nm. Simulations were performed in FDTD (Finite Difference Time

Domain - Lumerical software). The total computational window was chosen to be  $2 \times 2 \times 1.4 \mu\text{m}^3$  along the X, Y, and Z directions, respectively. A 1 nm fine mesh of  $200 \times 100 \times 100 \text{ nm}^3$  in the X, Y, and Z directions was used for the area surrounding the dipole and magnetic monopole nanoantennas. An incident plane wave ( $\lambda = 800 \text{ nm}$ ), polarized perpendicular to the long axis of the nanoslits (i.e., along Y) generated at 700 nm below the gold layer, propagates in the positive Z direction (figure 2 b,d). The lengths of the nanoslits were chosen so that these photonic antennas resonate at a wavelength of 800 nm (see Figure S1 of the supporting information for the influence of the geometrical parameters on the antenna resonance). This behavior is not limited to gold nanostructures and near-infrared wavelengths, but by using other plasmonic materials such as silver and aluminum, it is possible to develop magnetic monopole antennas at visible wavelengths (see Figures S2-3 in the Supporting information) and using longer antennas, telecommunication wavelengths are also reachable (see Figure S4 in the Supporting information).

Figure 3 presents the spectral response of these two magnetic antennas. In particular, it shows the increase of the local magnetic field at the surface of these antennas 10 nm from their ends and in the middle of the gold layer, as represented by the black star in the inset. From these spectral responses, it can be seen that these structures resonate at 800 nm wavelength and that the local magnetic field is increased by 12 and 6, respectively, for a dipole of length 140 nm and monopole of length 57 nm. In addition, we note a lower quality factor in the case of the magnetic monopole, indicating a faster dissipation of the energy of this antenna compared to the magnetic dipole, i.e. a high radiation efficiency.

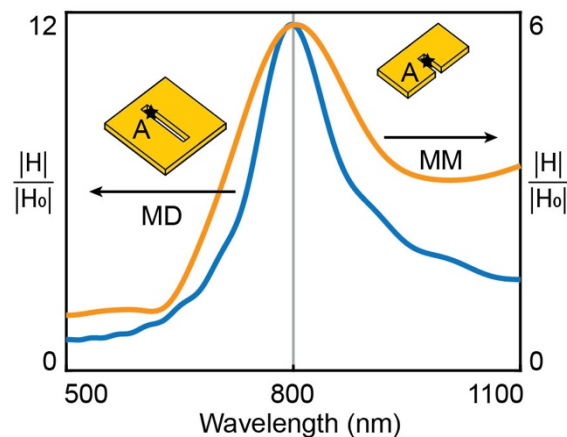


**Figure 3.** Magnetic spectral responses. Near-field spectral responses of the increase in optical magnetic field for the magnetic dipole nanoantenna (blue curve) and for the magnetic monopole nanoantenna (orange curve) at the position symbolized by the black star, at a position 10 nm from the end of the nanoslits and in the Z-center of the gold nanostructures.

To further detail the electromagnetic behavior of these antennas, the distributions of the electric and magnetic field enhancements in different planes of these structures are shown in Figure 4. In particular, the distributions of the electric (Fig. 4a,c,f,h) and magnetic (Fig. 4b,d,g,i) fields for the magnetic dipole (Fig. 4a-d) and the magnetic monopole (Fig. 4f-i) in the XY plane at the Z-center of the antennas (Fig. 4a,b,f,g) and the XZ plane at the Y-center of the antennas (Fig. 4c,d,h,i), are shown. As one can see, the magnetic dipole localizes the electric field inside the nanoslit and the magnetic field at both ends. This behavior is typical of a magnetic dipole antenna, as previously reported.<sup>47</sup> Furthermore, we can notice a substantial increase of the electric and magnetic field amplitudes in the near field, particularly by a factor of 30 and 14, respectively. On the other hand, the spatial distribution of the optical fields around the magnetic monopole antenna is very different; we observe that the latter appears truncated compared to the magnetic dipole, with only one magnetic and one electric hot spot, at each end of the nanoantenna. Also, we can observe that the amplitudes of the fields in the case of the monopole are divided by two compared to the magnetic dipole. These results indicate that the half-nanoslit behaves as half of a magnetic dipole with only one pole and therefore forming a magnetic monopole.

To investigate this phenomenon further, figures 4e and j provide the magnetic field lines in each of the antennas in an XZ plane at the Y-center of the nanostructures and at an arbitrary time  $t$ . In the case of the magnetic dipole, at the ends of the antenna where the magnitude of the magnetic field is the highest, the orientation of the field lines is opposite (Figure 4e), with on one side an orientation towards positive Z (left) and on the other side towards negative Z (right). These two orientations can be seen as the north and south poles of the magnetic dipole antenna. On the other hand, in the monopole case, we have only one orientation of the magnetic field lines (figure 4j) at the position of the hot spot shown in figure 4i. Therefore, the antenna described in figures 4f-j behaves like an antenna with only one pole, i.e., like a magnetic monopole antenna.

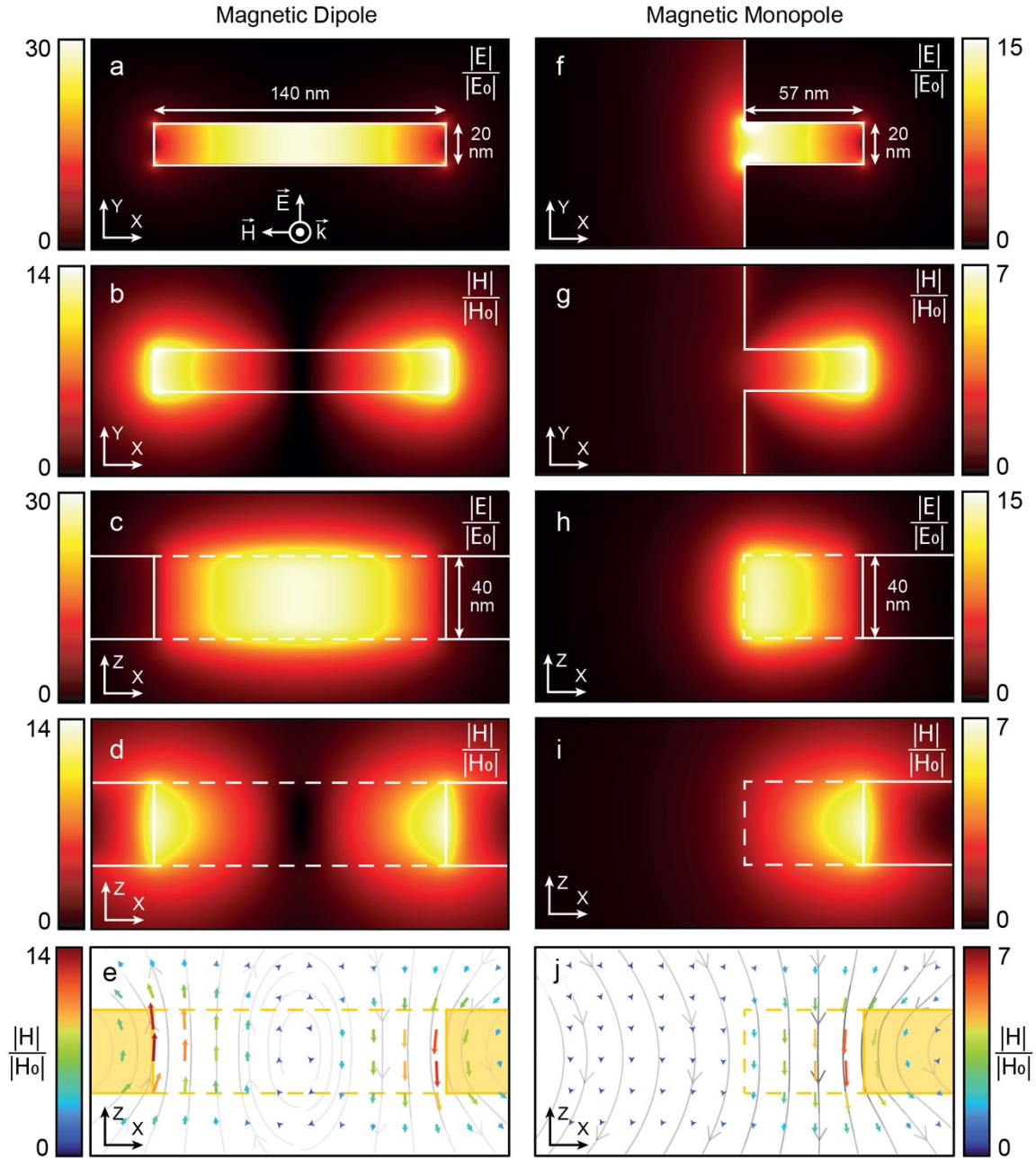


**Figure 4.** Spatial distributions of electric and magnetic fields in the near field. Spatial distributions of the (a,c,f,h) electric and (b,d,g,i) magnetic fields for the (a-d) magnetic dipole and (f-i) magnetic monopole antenna in an (a,b,f,g) XY plane at the Z-center of the nanostructures and in a (c,d,h,i) XZ plane at the Y-center of the nanoantennas. Field lines, amplitudes, and vector distributions of the optical magnetic field for e) the magnetic dipole and j) the magnetic monopole in an XZ plane at the Y-center of the structures. The yellow parts indicate the position of the nanoantennas.

Moreover, this magnetic monopole being an electromagnetic antenna, the orientation of the magnetic field lines oscillates in time so that the orientation of the magnetic field changes accordingly at the same frequency. For instance, this means that the pole of this antenna



alternates between south and north as shown in Figure 5. In this figure, the lines, the vector orientation, and the amplitude of the magnetic field are shown as a function of time at six equidistant moments of an optical cycle (see the full video online). We observe that the magnetic field amplitude oscillates over time, passing through maxima and minima. Also, as expected, the two extrema present in each optical cycle are oriented in opposite ways, one being oriented toward the positive Z, which can be called north, and the other towards the negative Z, which is south. Therefore, we have a north-south fluctuation in the orientation of this pole and, thus, an oscillating magnetic monopole nanoantenna.

We can also observe that the magnetic field lines, shown as gray lines in Figure 5, never loop back on themselves as observed for a magnetic dipole in Figure 4j. This behavior is yet another strong indication that our antenna behaves like a magnetic monopole. In addition, these field lines rotate around the magnetic hotspot generated by the magnetic monopole antenna.

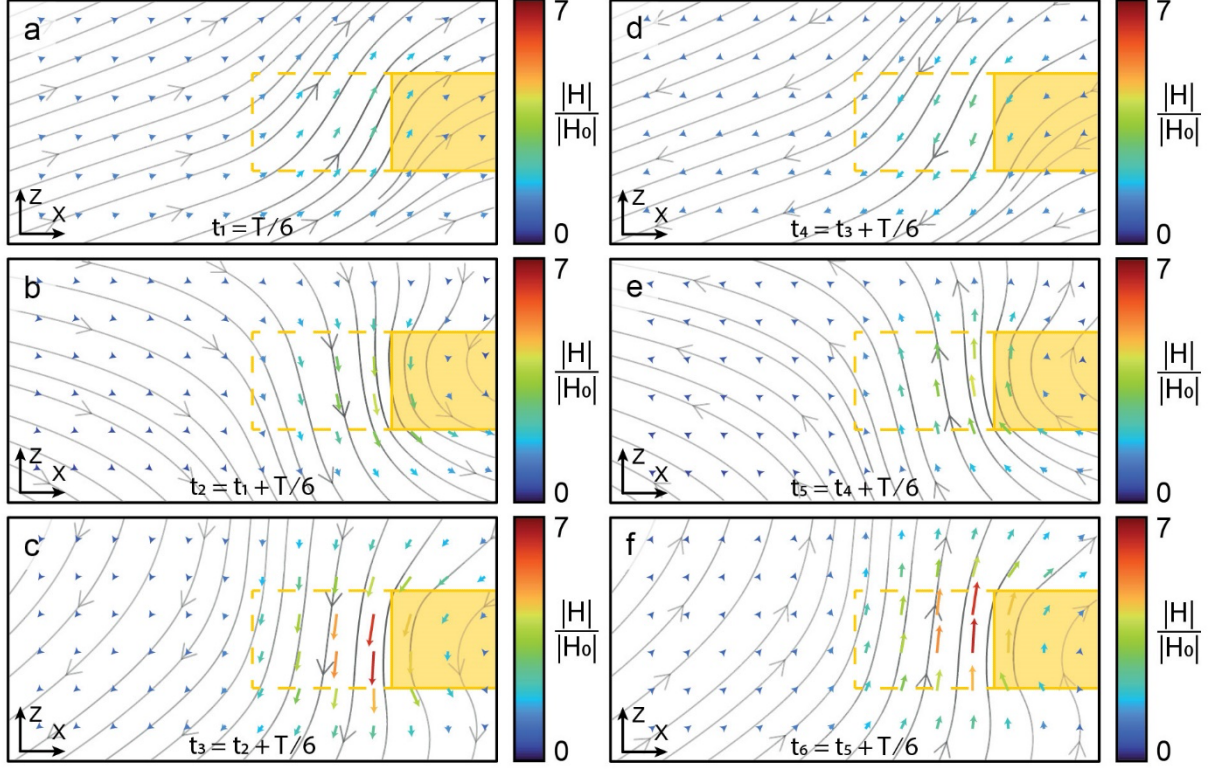


**Figure 5.** Temporal study of the  $\mathbf{H}$ -field vectorial distribution. Field lines, amplitudes, and vector distributions of the magnetic field in an XZ plane at the Y-center of the magnetic monopole at different times of a single optical cycle (the time is indicated in each figure). The yellow parts indicate the position of the monopole antenna.

To further highlight how the behavior of a half-nanoslit antenna is associated with the presence of a single magnetic pole, we propose to compute an effective magnetic charge,  $Q_m$ , in analogy with electric monopoles that exist due to the presence of a single electric charge (Figure 1). It is indeed possible to formulate Gauss's law of magnetism in terms of the magnetic field strength  $\mathbf{H}$  instead of the magnetic field flux density  $\mathbf{B}$  as:

$$\oiint \mu_0 \mathbf{H} \cdot d\mathbf{S} = Q_m(1)$$

Where  $\mathbf{H}$  is the magnetic field strength,  $\mu_0$  is the vacuum permeability,  $d\mathbf{S}$  the surface element, and  $Q_m$  is an effective magnetic charge, homogeneous to a magnetic flux. This definition of  $Q_m$  remains fully compatible with Maxwell's equations, which state that the divergence of the magnetic induction  $\mathbf{B}$  must be equal to 0 in the absence of true magnetic charges (hence the term of effective magnetic charge used here), simply by introducing a magnetization  $\mathbf{M}$  due to the antenna as  $\mathbf{B} = \mu_0(\mathbf{H} + \mathbf{M})$ .

Since the magnetic monopole is an oscillating antenna, we can calculate the evolution of this integral over time. Figure 6e shows the evolution of  $Q_m$  over an oscillation period of time. As

one can see,  $Q_m$  is not zero and oscillates over time with the same periodicity as the incident wave. For the sake of comparison, the exact same calculation is carried out for each pole of the magnetic dipole antenna (Figure 6b,c) and the dipole antenna as a whole (Figure 6d). In that case, taken separately, the magnetic charges of each pole oscillate in the same way and with the same periodicity as the magnetic monopole, with a phase shift of  $\pi$  concerning the pole of opposite symmetry (Figure 6e). However, when computing the effective magnetic charge over the entire dipole antenna, we find that  $Q_m$  is zero as expected (Figure 6e and f). Zooming in on the temporal behavior of  $Q_m$  in the case of the dipole antenna, we can clearly see that the signal is made up entirely of numerical noise (Figure 6f).

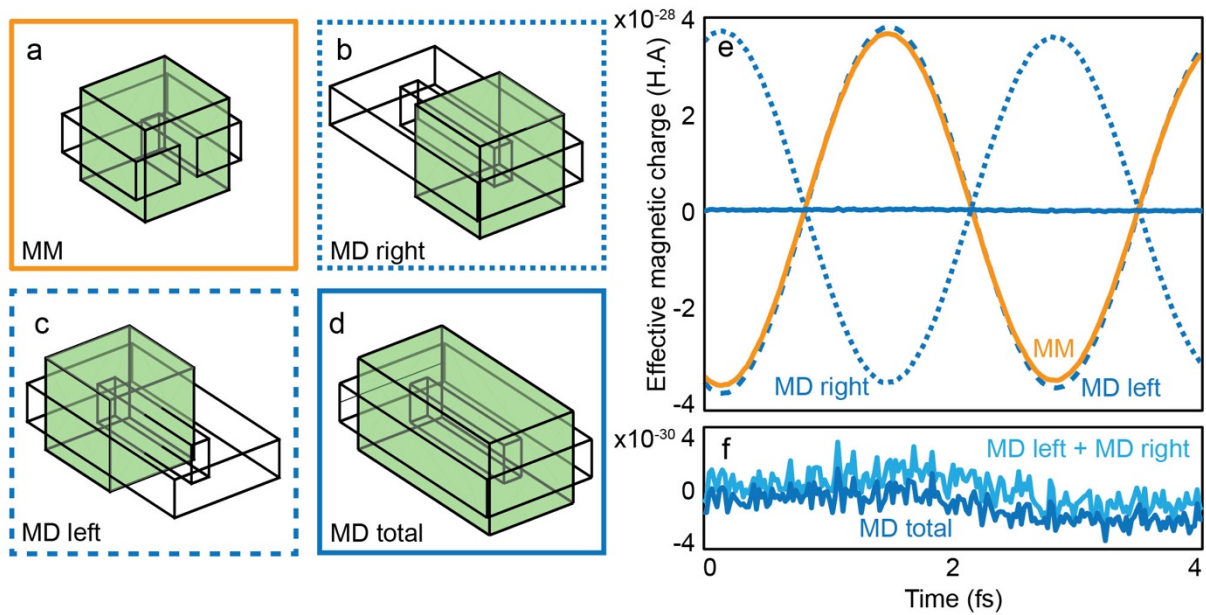


**Figure 6.** Calculation of the effective magnetic charges generated by the magnetic monopole and dipole antennas for a planewave excitation with  $E=1V/m$ . a-d) Schematic representation of the surfaces considered (green parallelepiped) for the calculation of Gauss's law, for a) the magnetic monopole, b,c) the two poles of the magnetic dipole, and d) the magnetic dipole as a whole. e) Effective magnetic charges calculated for these different antennas over time. Curve colors and continuities correspond to the panels in a-d). f) A zoom in of the two poles taken together of the magnetic dipole antenna.

The calculation of this non-zero flux of the magnetic field strength, or effective magnetic charge  $Q_m$ , is thus further proof that our antenna does indeed behave like a magnetic monopole (see Figure S5 of the Supporting Information for the case of the electric monopole and electric dipole antennas). Furthermore, the ability of magnetic monopole antennas to locally create a non-zero value of  $Q_m$  indicates that they are interesting building blocks to manipulate the relative permeability  $\mu$ . Indeed, if  $\mu$  can be defined as  $\mathbf{B}=\mu_0.\mu.\mathbf{H}$ , and considering that the flux

of  $\mathbf{B}$  is zero, then equation (1) implies that  $\mu$  must be different from 1 in the case of the magnetic monopole antenna while it remains equal to 1 for a magnetic dipole antenna. This is an appealing observation since it suggests that, just as metamaterials made up of antenna arrays manipulate effective permittivity and permeability in order, for example, to create negative-index materials,<sup>50, 51</sup> a magnetic monopole modulates the permeability at the single-antenna level, opening up new prospects for the engineering of effective optical constants by photonic nanostructures.

Finally, to demonstrate the versatility of this new type of antenna in terms of materials and resonant frequency range, Figure 7 shows the spectral response of a monopole antenna fabricated in a copper foil with millimeter dimensions (Figure 7a). For these dimensions, the monopole resonates at GHz frequencies (Figure 7b). Also, as shown in Figure 7c, by changing the length of this antenna, it is possible to tune its resonant wavelength over several GHz. Figure 7b also shows that several modes co-exist. The first, at 1.5 GHz, corresponds to a magnetic monopole, as shown by the magnetic field distribution in Figure 7d. The second and third modes correspond to higher-order modes (Figure 7e,f), in this case, half poles of order 8 and 12 (see Figure S4 for a description of this multipolar effect at optical frequencies). These results demonstrate the potential of this new type of magnetic monopole antenna at low frequencies, with direct applications such as magnetic resonance imaging.

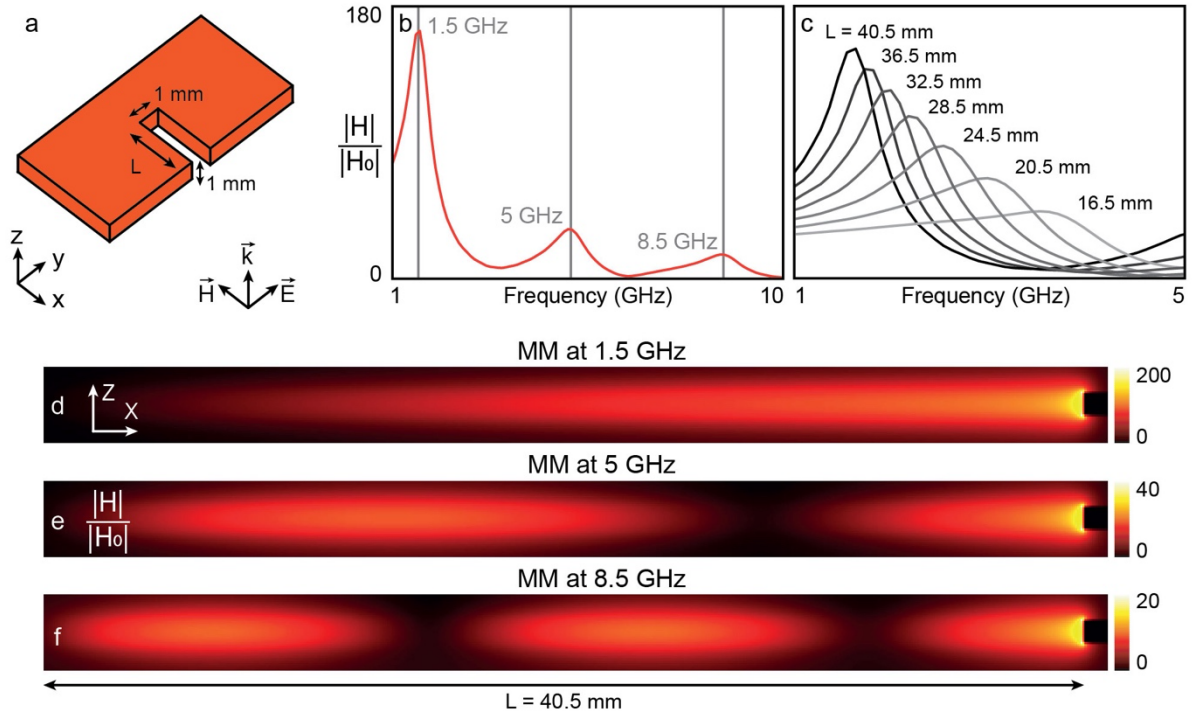


**Figure 7.** Study of a copper monopole antenna at gigahertz frequencies. a) Dimensions of the monopole antenna in a copper foil. The width of the slit is 1 mm, the thickness of the foil is also 1 mm, and the length of the monopole varies. b) Spectral response of the 40.5 mm long monopole excited by a plane wave polarized as shown in a) and centered at the 5GHz frequency. The spectrum is calculated at 0,25 mm from the metal, at the end of the monopole, and the Z-center of the antenna. c) Spectral responses for different monopole lengths. d-e) Normalized magnetic field distribution at the Z-center of the 40.5 mm long monopole for the resonance wavelengths identified in b) and in XZ plane.

## Conclusion

In conclusion, we demonstrated that a half-nanoslit carved in a thin semi-infinite gold layer behaves as a magnetic monopole antenna. We showed that the latter allows the generation of a single magnetic hot spot where the optical magnetic field is enhanced. Furthermore, by studying the field lines within this locally enhanced magnetic energy density, we established that the vectorial distribution corresponds to a single pole, validating the monopole character of this antenna. Also, by studying the temporal response of this system, we showed that the magnetic vectorial distribution alternated between north-south orientations over time due to the electromagnetic character of this magnetic monopole, thus allowing this antenna to radiate its energy efficiently in the far field. Finally, using a Gauss's law of magnetism applied to the magnetic field strength on a closed surface surrounding this antenna, we demonstrated the presence of an effective magnetic charge within it, demonstrating even further the magnetic

monopole behavior of this antenna and opening up new perspectives in locally manipulating the effective permeability of the material.

In addition to this antenna's new model for magnetic monopoles, this research also opens the way to generating intense magnetic hot spots, free of any electric field, to couple magnetic light to matter<sup>52</sup> efficiently. In particular, topics strongly dependent on the magnetic component of light will directly benefit from this type of system. Finally, although the present study is mainly performed at optical wavelengths, the extension of this type of antenna to lower frequencies opens new possibilities in terms of applications, such as magnetic resonance imaging.<sup>53</sup>

## **Funding sources**

This work is supported by the Agence Nationale de la Recherche (ANR-20-CE09-0031-01 and ANR-22-CE09-0027-04), the Institut de Physique du CNRS (Tremplin@INP 2020) and the China Scholarship Council.

**Conflict of interest statement:** The authors declare no conflict of interest regarding this article.

## **Supporting Information**

Additional information about the influence of geometric parameters on the resonance of the magnetic monopole antenna, electric and magnetic dipoles and monopoles in other plasmonic materials, the study of magnetic monopole and dipole antennas in the case of a perfect electric conductor material, the multimodal study of the monopole antenna, and the calculation of the electric charge generated by the electric monopole.

## References

- (1) Dirac, P. A. M. Quantised singularities in the electromagnetic field. *Proceedings of the Royal Society of London. Series A, Containing Papers of a Mathematical and Physical Character* **1931**, 133 (821), 60-72.
- (2) Preskill, J. Magnetic monopoles. *Annu. Rev. Nucl. Part. Sci.* **1984**, 34 (1), 461-530.
- (3) Goldhaber, A. S.; Trower, W. P. Resource Letter MM-1: Magnetic monopoles. *American Journal of Physics* **1990**, 58 (5), 429-439.
- (4) Patrizzii, L.; Spurio, M. Status of searches for magnetic monopoles. *Annu. Rev. Nucl. Part. Sci.* **2015**, 65, 279-302.
- (5) Tokura, Y.; Yasuda, K.; Tsukazaki, A. Magnetic topological insulators. *Nature Reviews Physics* **2019**, 1 (2), 126-143.
- (6) Castelnovo, C.; Moessner, R.; Sondhi, S. L. Magnetic monopoles in spin ice. *Nature* **2008**, 451 (7174), 42-45.
- (7) Baskaran, G.; Anderson, P. W. Gauge theory of high-temperature superconductors and strongly correlated Fermi systems. *Phys. Rev. B* **1988**, 37 (1), 580.
- (8) Gould, O.; Rajantie, A. Magnetic monopole mass bounds from heavy-ion collisions and neutron stars. *Phys. Rev. Lett.* **2017**, 119 (24), 241601.
- (9) Wen, X.-G.; Zee, A. Neutral superfluid modes and “magnetic” monopoles in multilayered quantum Hall systems. *Phys. Rev. Lett.* **1992**, 69 (12), 1811.
- (10) Kanazawa, N.; Seki, S.; Tokura, Y. Noncentrosymmetric magnets hosting magnetic skyrmions. *Advanced Materials* **2017**, 29 (25), 1603227.
- (11) Lavrentovich, O. D. Topological defects in dispersed words and worlds around liquid crystals, or liquid crystal drops. *Liq. Cryst.* **1998**, 24 (1), 117-126.
- (12) Ünzelmann, M.; Bentmann, H.; Figgemeier, T.; Eck, P.; Neu, J.; Geldiyev, B.; Diekmann, F.; Rohlf, S.; Buck, J.; Hoesch, M. Momentum-space signatures of Berry flux monopoles in the Weyl semimetal TaAs. *Nat. Commun.* **2021**, 12 (1), 3650.
- (13) Kanazawa, N.; Nii, Y.; Zhang, X.-X.; Mishchenko, A.; De Filippis, G.; Kagawa, F.; Iwasa, Y.; Nagaosa, N.; Tokura, Y. Critical phenomena of emergent magnetic monopoles in a chiral magnet. *Nat. Commun.* **2016**, 7 (1), 11622.
- (14) Weiner, M. M. *Monopole antennas*; CRC Press, 2003.
- (15) Taminiau, T. H.; Moerland, R. J.; Segerink, F. B.; Kuipers, L.; van Hulst, N. F.  $\lambda/4$  resonance of an optical monopole antenna probed by single molecule fluorescence. *Nano. Lett.* **2007**, 7 (1), 28-33.
- (16) Liang, Z.; Li, Y.; Liu, J.; Zheng, S. Y.; Long, Y. Microstrip magnetic monopole endfire array antenna with vertical polarization. *IEEE Transactions on Antennas and Propagation* **2016**, 64 (10), 4208-4217.
- (17) Liang, Z.; Li, Y.; Feng, X.; Liu, J.; Qin, J.; Long, Y. Microstrip magnetic monopole and dipole antennas with high directivity and a horizontally polarized omnidirectional pattern. *IEEE Transactions on Antennas and Propagation* **2018**, 66 (3), 1143-1152.

- (18) Karaveli, S.; Zia, R. Spectral tuning by selective enhancement of electric and magnetic dipole emission. *Phys. Rev. Lett.* **2011**, *106* (19), 193004.
- (19) Kuznetsov, A. I.; Miroschnichenko, A. E.; Fu, Y. H.; Zhang, J.; Luk'Yanchuk, B. Magnetic light. *Scientific reports* **2012**, *2*, 492.
- (20) Aigouy, L.; Cazé, A.; Gredin, P.; Mortier, M.; Carminati, R. Mapping and quantifying electric and magnetic dipole luminescence at the nanoscale. *Phys. Rev. Lett.* **2014**, *113* (7), 076101.
- (21) Kasperczyk, M.; Person, S.; Ananias, D.; Carlos, L. D.; Novotny, L. Excitation of magnetic dipole transitions at optical frequencies. *Phys. Rev. Lett.* **2015**, *114* (16), 163903.
- (22) Mivelle, M.; Grosjean, T.; Burr, G. W.; Fischer, U. C.; Garcia-Parajo, M. F. Strong Modification of Magnetic Dipole Emission through Diabolo Nanoantennas. *ACS Photonics* **2015**, *2* (8), 1071-1076.
- (23) Rabouw, F. T.; Prins, P. T.; Norris, D. J. Europium-Doped NaYF<sub>4</sub> Nanocrystals as Probes for the Electric and Magnetic Local Density of Optical States throughout the Visible Spectral Range. *Nano. Lett.* **2016**, *16* (11), 7254-7260.
- (24) Erndes, C.; Lin, H.-J.; Mortier, M.; Gredin, P.; Mivelle, M.; Aigouy, L. Exploring the magnetic and electric side of light through plasmonic nanocavities. *Nano. Lett.* **2018**, *18* (8), 5098-5103.
- (25) Sanz-Paz, M.; Erndes, C.; Esparza, J. U.; Burr, G. W.; van Hulst, N. F.; Maitre, A. s.; Aigouy, L.; Gacoin, T.; Bonod, N.; Garcia-Parajo, M. F.; et al. Enhancing Magnetic Light Emission with All-Dielectric Optical Nanoantennas. *Nano. Lett.* **2018**, *18* (6), 3481-3487.
- (26) Vaskin, A.; Mashhadi, S.; Steinert, M.; Chong, K. E.; Keene, D.; Nanz, S.; Abass, A.; Rusak, E.; Choi, D.-Y.; Fernandez-Corbaton, I.; et al. Manipulation of magnetic dipole emission from Eu<sup>3+</sup> with Mie-resonant dielectric metasurfaces. *Nano. Lett.* **2019**, *19* (2), 1015-1022.
- (27) Reynier, B.; Charron, E.; Markovic, O.; Yang, X.; Gallas, B.; Ferrier, A.; Bidault, S.; Mivelle, M. Full control of electric and magnetic light-matter interactions through a plasmonic nanomirror on a near-field tip. Submission date : 2023-01-23. *Optica* **2023**, *10* (5). <https://doi.org/10.1364/OPTICA.486207>. Accessed 2023-05-03.
- (28) Poulidakos, L. V.; Gutsche, P.; McPeak, K. M.; Burger, S.; Niegemann, J.; Hafner, C.; Norris, D. J. Optical chirality flux as a useful far-field probe of chiral near fields. *ACS photonics* **2016**, *3* (9), 1619-1625.
- (29) Garcia-Guirado, J.; Svedendahl, M.; Puigdollers, J.; Quidant, R. Enhanced chiral sensing with dielectric nanoresonators. *Nano. Lett.* **2019**, *20* (1), 585-591.
- (30) Both, S.; Schäferling, M.; Sterl, F.; Muljarov, E. A.; Giessen, H.; Weiss, T. Nanophotonic chiral sensing: how does it actually work? *ACS Nano* **2022**, *16* (2), 2822-2832.
- (31) Manjavacas, A.; Fenollosa, R.; Rodriguez, I.; Jiménez, M. C.; Miranda, M. A.; Meseguer, F. Magnetic light and forbidden photochemistry: the case of singlet oxygen. *Journal of Materials Chemistry C* **2017**, *5* (45), 11824-11831.
- (32) Lee, C.; Xu, E. Z.; Liu, Y.; Teitelboim, A.; Yao, K.; Fernandez-Bravo, A.; Kotulska, A. M.; Nam, S. H.; Suh, Y. D.; Bednarkiewicz, A. Giant nonlinear optical responses from photon-avalanching nanoparticles. *Nature* **2021**, *589* (7841), 230-235.
- (33) Milligan, T. A. *Modern antenna design*; John Wiley & Sons, 2005.



- (34) Novotny, L.; van Hulst, N. Antennas for light. *Nat. Photonics* **2011**, *5* (2), 83-90.
- (35) Bonod, N.; Bidault, S.; Burr, G. W.; Mivelle, M. Evolutionary Optimization of All-Dielectric Magnetic Nanoantennas. *Advanced Optical Materials* *0* (0), 1900121. DOI: 10.1002/adom.201900121.
- (36) Kuznetsov, A. I.; Miroshnichenko, A. E.; Brongersma, M. L.; Kivshar, Y. S.; Luk'yanchuk, B. Optically resonant dielectric nanostructures. *Science* **2016**, *354* (6314), aag2472.
- (37) Wiecha, P. R.; Arbouet, A.; Girard, C.; Lecestre, A.; Larrieu, G.; Paillard, V. Evolutionary multi-objective optimization of colour pixels based on dielectric nanoantennas. *Nat. Nanotechnol.* **2017**, *12* (2), 163.
- (38) Bidault, S.; Mivelle, M.; Bonod, N. Dielectric nanoantennas to manipulate solid-state light emission. *J. Appl. Phys.* **2019**, *126* (9), 094104.
- (39) Anger, P.; Bharadwaj, P.; Novotny, L. Enhancement and quenching of single-molecule fluorescence. *Phys. Rev. Lett.* **2006**, *96* (11), 113002.
- (40) Kühn, S.; Håkanson, U.; Rogobete, L.; Sandoghdar, V. Enhancement of single-molecule fluorescence using a gold nanoparticle as an optical nanoantenna. *Phys. Rev. Lett.* **2006**, *97* (1), 017402.
- (41) Punj, D.; Mivelle, M.; Moparthi, S. B.; van Zanten, T. S.; Rigneault, H.; van Hulst, N. F.; García-Parajó, M. F.; Wenger, J. A plasmonic/antenna-in-box/platform for enhanced single-molecule analysis at micromolar concentrations. *Nat. Nanotechnol.* **2013**.
- (42) Baffou, G.; Quidant, R. Thermo-plasmonics: using metallic nanostructures as nano-sources of heat. *Laser & Photonics Reviews* **2013**, *7* (2), 171-187.
- (43) Mazouzi, Y.; Sallem, F.; Farina, F.; Loiseau, A.; Tartaglia, N. R.; Fontaine, M.; Parikh, A.; Salmain, M.; Neri, C.; Boujday, S. Biosensing Extracellular Vesicle Subpopulations in Neurodegenerative Disease Conditions. *ACS sensors* **2022**, *7* (6), 1657-1665.
- (44) Curto, A. G.; Volpe, G.; Taminiau, T. H.; Kreuzer, M. P.; Quidant, R.; van Hulst, N. F. Unidirectional emission of a quantum dot coupled to a nanoantenna. *Science* **2010**, *329* (5994), 930-933.
- (45) Fromm, D. P.; Sundaramurthy, A.; Schuck, P. J.; Kino, G.; Moerner, W. Gap-dependent optical coupling of single "bowtie" nanoantennas resonant in the visible. *Nano. Lett.* **2004**, *4* (5), 957-961.
- (46) Martin, J.; Kociak, M.; Mahfoud, Z.; Proust, J.; Gérard, D.; Plain, J. High-resolution imaging and spectroscopy of multipolar plasmonic resonances in aluminum nanoantennas. *Nano. Lett.* **2014**, *14* (10), 5517-5523.
- (47) Singh, A.; Calbris, G.; van Hulst, N. F. Vectorial Nanoscale Mapping of Optical Antenna Fields by Single Molecule Dipoles. *Nano. Lett.* **2014**, *14* (8), 4715-4723.
- (48) Curto, A. G. Optical antennas control light emission. Universitat Politècnica de Catalunya, 2014.
- (49) Park, Y.; Kim, J.; Roh, Y.-G.; Park, Q.-H. Optical slot antennas and their applications to photonic devices. *Nanophotonics* **2018**, *7* (10), 1617-1636.
- (50) Shelby, R. A.; Smith, D. R.; Schultz, S. Experimental verification of a negative index of refraction. *science* **2001**, *292* (5514), 77-79.

(51) Schurig, D.; Mock, J. J.; Justice, B.; Cummer, S. A.; Pendry, J. B.; Starr, A. F.; Smith, D. R. Metamaterial electromagnetic cloak at microwave frequencies. *Science* **2006**, *314* (5801), 977-980.

(52) Baranov, D. G.; Savelev, R. S.; Li, S. V.; Krasnok, A. E.; Alù, A. Modifying magnetic dipole spontaneous emission with nanophotonic structures. *Laser & Photonics Reviews* **2017**, *11* (3), 1600268.

(53) Uğurbil, K.; Adriany, G.; Andersen, P.; Chen, W.; Garwood, M.; Gruetter, R.; Henry, P.-G.; Kim, S.-G.; Lieu, H.; Tkac, I. Ultrahigh field magnetic resonance imaging and spectroscopy. *Magnetic resonance imaging* **2003**, *21* (ARTICLE), 1263-1281.

## Table of Contents

